Electromagnetically-induced-transparency plasmonics: Quantum-interference-assisted tunable surface-plasmon-polariton resonance and excitation

Jian Qi Shen*

Centre for Optical and Electromagnetic Research, State Key Laboratory of Modern Optical Instrumentations, East Building No. 5, Zijingang Campus, Zhejiang University, Hangzhou 310058, The People's Republic of China

and Zhejiang Provincial Key Laboratory for Sensing Technologies, Joint Research Centre of Photonics of the Royal Institute of Technology (Sweden) and Zhejiang University, Zijingang Campus, Zhejiang University, Hangzhou 310058, The People's Republic of China

(Received 18 December 2013; published 11 August 2014)

An experimentally feasible configuration of a prism coupler with an electromagnetically-induced-transparency (EIT) medium layer, e.g., a semiconductor-quantum-dot (SQD) medium, deposited upon its prism base is suggested for generating tunable surface-plasmon-polariton resonance. Such surface-plasmon-polariton resonance and optical excitation of a surface plasmon wave can be manipulated by switchable quantum interference among SQD multilevel transitions driven by two external control fields. When an incident probe field is coupled into a surface plasmon wave excitation mode, the surface-plasmon-polariton (SPP) resonance at the interface between the SQD medium layer and the substrate will arise, and the quantum-coherently controllable reflection spectrum of the probe field on the prism base can be achieved. In this process, *destructive* and *constructive* quantum interference (determined by the intensity ratio of the two external control fields) in the SQD multilevel system plays a key role for achieving the tunable reflection spectrum. The EIT-based surface-plasmon-polariton resonance presented here will have three characteristics (some of them would be attractive): (i) switchable quantum interference exhibited by surface plasmon wave excitation, (ii) quantum-coherently controllable surface plasmon polaritons by external optical fields, (iii) surface wave sensitive to dispersion of the SQD quantum coherent medium. Such an effect of controllable optical response based on the *quantum-interference switchable surface-plasmon-polariton resonance* in the EIT-prism coupler may find some potential applications in design of new photonic and quantum optical devices.

DOI: 10.1103/PhysRevA.90.023814 PACS number(s): 42.50.Gy, 42.50.Nn

I. INTRODUCTION

Over the past two decades, intensive attention has been paid to the topics of quantum coherence, e.g., atomic phase coherence [1–4], which can coherently control light with light. Such quantum coherence in multilevel atomic systems has exhibited many interesting phenomena, e.g., electromagnetically induced transparency (EIT) [3], light amplification without inversion [5], spontaneous emission cancellation [6], multiphoton population trapping [7] as well as quantum-coherent left-handed media [8]. Most of these effects and phenomena have been found in various three-level coherent systems [3]. It should be noted that a four-level system that is driven by two control fields and one probe field can manipulate the optical response of a quantum coherent medium (semiconductor-quantum-dot material or alkali metallic atomic vapor) with nontrivial *destructive* and *constructive* quantum interference between the two transitions that are driven by two applied control fields [9–13]. Therefore, an effect of tunable double-control EIT would be realized through quantum interference between the transition pathways excited by the two external control fields.

In the literature, an effect called ATR (attenuated total reflection) for exciting surface plasmon waves in metal optics has been observed in Otto and Kretschmann's configurations (prism couplers) [14–17], where the intensity of a p-polarized (TM) reflected wave exhibits a sharp dip when the angle of incidence at an interface between a prism and a thin metal film is larger than the critical angle for total reflection [18]. Such a sudden drawdown in reflectance is caused by the drastic coupling of incident waves into surface-plasmon-polariton (SPP) modes in the thin metal layer. The ATR technique has been a powerful tool for determining metal characteristics (e.g., dielectric function and film thickness) [16,19,20]. Both SPP resonance and localized surface plasmon resonance (SPR) have become fundamental mechanisms for many optical devices (e.g., optical sensors and modulators [21,22]) and biomolecular sensors [23]. Recently, surface plasmon wave excitation and SPR polaritons have captured much interest in optics, photonics, electronics, and related technologies [24–26], since it can exhibit a strong interaction with nanoscopic objects, and would have many intriguing applications for designing new micro- and nanoscale photonic devices [24–26].

In order to realize dispersion-sensitive and intensity-tunable (i.e., depending upon the applied external fields) surface-plasmon-polariton resonance and excitation by taking full advantage of quantum coherence (e.g., quantum interference between multilevel transitions), we shall here suggest an experimentally feasible scheme for an EIT-prism coupling system [see Fig. 1(a) for its schematic diagram], in which an incident probe wave that can be coupled into surface plasmon wave modes will be dramatically influenced by the *destructive* and *constructive* quantum interference between the $|c\rangle$-$|a\rangle$ and $|c'\rangle$-$|a\rangle$ transitions driven by the two control fields [see Fig. 1(b)]. Thus, a quantum-interference switchable reflection spectrum of the prism coupler [see Fig. 1(a)] can be coherently

*jqshen@zju.edu.cn

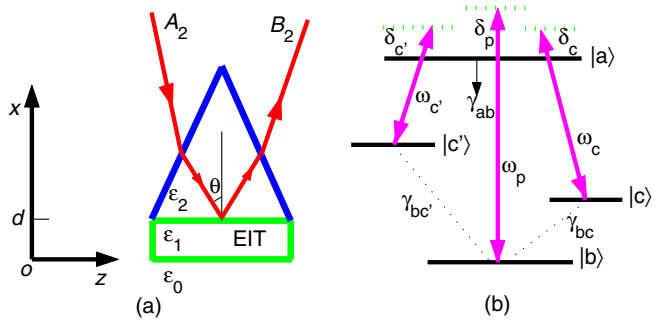

FIG. 1. (Color online) The schematic diagrams of an EIT-prism coupler (a) and a four-level quantum coherent (EIT) system driven by two strong control fields and one weak probe field (b). (a) The probe wave (denoted by A_2) is incident and then reflected on the prism base, i.e., the interface (at $x = d$) between the prism dielectric and a thin EIT layer (e.g., a quantum-dot thin film). (b) The two control fields excite the $|c\rangle$-$|a\rangle$ and $|c'\rangle$-$|a\rangle$ transitions, respectively. The $|b\rangle$-$|a\rangle$ transition (driven by the probe wave) can be controllably manipulated via the destructive and constructive quantum interference between the $|c\rangle$-$|a\rangle$ and $|c'\rangle$-$|a\rangle$ transitions. If the destructive quantum interference between the $|c\rangle$-$|a\rangle$ and $|c'\rangle$-$|a\rangle$ transitions occurs, the two levels $|c\rangle$ and $|c'\rangle$ seem to be absent, and then the four-level system $\{|a\rangle,|b\rangle,|c\rangle,|c'\rangle\}$ will be equivalent to a two-level one $\{|a\rangle,|b\rangle\}$.

controlled by the intensity ratio of the two external control fields, that is, whether it is the *destructive* or *constructive* quantum interference is determined by the intensity ratio of the two external control fields (to be addressed in the next section). In the literature [27–29], the quantum coherence, including electromagnetically induced transparency, in three- and four-level systems in quantum dots has been studied both theoretically and experimentally. The idea in our model for treating the optical characteristics of the four-level quantum dot medium layer in Fig. 1(b) is suggested based on these references [27–29].

Very recently, there has been an advance of *quantum-dot plasmonics*, i.e., surface plasmon resonance demonstrated in semiconductor quantum dots [30–32]. As we know, in general, plasmonic resonance in nanometer-scale particles has often been limited to noble metals [30]. Recent work shows that such metal plasmonics can be generalized to semiconductor quantum-dot (SQD) plasmonics (in, e.g., copper-chalcogenide quantum dots and metal-oxide-based quantum dots) [30–32]. Although it is simply the localized plasmon resonance in plasmonic QDs, it would offer a possibility of surface-plasmon-polariton resonance in a collection of QDs [the SQD medium layer in Fig. 1(a)].

In the sections that follow, we shall treat the tunable reflection spectrum of the prism coupler, in which an SQD thin layer can exhibit destructive and constructive quantum interference in its four-level system. The surface plasmon wave and its optical excitation (quantum-interference tunable) are also addressed. The highly dispersion-sensitive surface-plasmon-polariton resonance and excitation will be pointed out, and the potential applications for new photonic device design will be discussed.

II. EIT PLASMONICS FOR SURFACE-PLASMON-POLARITON RESONANCE THROUGH QUANTUM COHERENT MANIPULATION OF MULTILEVEL INTERFERENCE

A. Four-level destructive and constructive quantum interference

In the present EIT-prism coupler for generating surface plasmon wave excitation, the quantum coherent medium layer (e.g., a thin semiconductor-quantum-dot material that can exhibit EIT effect under certain proper conditions) is deposited upon the prism base. In Fig. 1(b), the three frequency detunings δ_c, $\delta_{c'}$, and δ_p of the four-level EIT system are defined as follows: $\delta_c = \omega_c - \omega_{ac}$, $\delta_{c'} = \omega_{c'} - \omega_{ac'}$, and $\delta_p = \omega_p - \omega_{ab}$, where ω_{ac}, $\omega_{ac'}$, and ω_{ab} denote the energy-level transition frequencies, and ω_c, $\omega_{c'}$, ω_p represent the mode frequencies of the control and the probe beams, respectively. We suppose that the Rabi frequency Ω_p of the probe field is sufficiently weak (i.e., it is small compared with the other parameters such as γ_{ab},Ω_c and $\Omega_{c'}$), so that nearly all these four-level systems remain in the ground state [33]. Besides, the population ρ_{aa} of the upper level $|a\rangle$ almost vanishes because of the coherent population trapping [33]. Under these conditions, the equations of the three off-diagonal density matrix elements ρ_{cb},$\rho_{c'b}$,ρ_{ab} for the present tripod-configuration system are given by

$$\dot{\rho}_{ab} = -(\gamma_{ab} - i\delta_p)\rho_{ab} + \frac{i}{2}\Omega_c\rho_{cb} + \frac{i}{2}\Omega_{c'}\rho_{c'b} + \frac{i}{2}\Omega_p\rho_{bb},$$
$$\dot{\rho}_{cb} = -[\gamma_{bc} - i(\delta_p - \delta_c)]\rho_{cb} + \frac{i}{2}\Omega_c^*\rho_{ab},$$
$$\dot{\rho}_{c'b} = -[\gamma_{bc'} - i(\delta_p - \delta_{c'})]\rho_{c'b} + \frac{i}{2}\Omega_{c'}^*\rho_{ab}. \quad (1)$$

The complete equation set of the density matrix elements is presented in the appendix. The three Rabi frequencies in Eq. (1) are expressed by $\Omega_c = \wp_{cb}E_c/\hbar$, $\Omega_{c'} = \wp_{c'b}E_{c'}/\hbar$, and $\Omega_p = \wp_{ab}E_p/\hbar$ with $\wp_{cb}$, $\wp_{c'b}$, and $\wp_{ab}$ the transition-induced electric dipole moments, and E_c, $E_{c'}$, and E_p the electric field envelopes (slowly varying amplitudes) of the strong control beams and the weak probe field, respectively. The dynamical equations of the other off-diagonal density matrix elements such as ρ_{ac},$\rho_{ac'}$,$\rho_{cc'}$ are not taken into consideration, since, in general, these density matrix elements are negligibly small compared with ρ_{cb},$\rho_{c'b}$,ρ_{ab} that are intimately related to the two- or three-level dark state (consisting of the lower energy levels).

We shall discuss the effects of destructive and constructive quantum interference among the $|c\rangle$-$|a\rangle$ and $|c'\rangle$-$|a\rangle$ transitions, in which the two- or three-level dark state will be involved. For the steady solution, we have $\dot{\rho}_{cb} = 0$ and $\dot{\rho}_{c'b} = 0$, and we will have

$$\rho_{cb} = \frac{i}{2}\left[\frac{\Omega_c^*\rho_{ab}}{\gamma_{bc} - i(\delta_p - \delta_c)}\right],$$
$$\rho_{c'b} = \frac{i}{2}\left[\frac{\Omega_{c'}^*\rho_{ab}}{\gamma_{bc'} - i(\delta_p - \delta_{c'})}\right]. \quad (2)$$

Then from the first formula in Eq. (1), one can have the exact solution of ρ_{ab} (keeping $\dot{\rho}_{ab} = 0$ in mind when obtaining the

steady solution),

$$\rho_{ab} = \frac{\frac{i}{2}(\Omega_c \rho_{cb} + \Omega_{c'} \rho_{c'b} + \Omega_p \rho_{bb})}{\gamma_{ab} - i\delta_p}. \quad (3)$$

If we substitute Eq. (2) into the double-control destructive interference condition $\Omega_c \rho_{cb} + \Omega_{c'} \rho_{c'b} = 0$ between the two transitions $|c\rangle$-$|a\rangle$ and $|c'\rangle$-$|a\rangle$ driven by the two control fields, we can obtain

$$\begin{aligned} &\Omega_c \rho_{cb} + \Omega_{c'} \rho_{c'b} \\ &= \frac{i}{2}\left[\frac{\Omega_c^* \Omega_c}{\gamma_{bc} - i(\delta_p - \delta_c)} + \frac{\Omega_{c'}^* \Omega_{c'}}{\gamma_{bc'} - i(\delta_p - \delta_{c'})}\right]\rho_{ab} \\ &= 0. \end{aligned} \quad (4)$$

Note that the dephasing rates γ_{bc} and $\gamma_{bc'}$ are negligibly small compared with the spontaneous emission decay rates and the Rabi frequencies of the control fields. Then according to the condition of destructive quantum interference (4), we shall have the following relation:

$$\frac{\Omega_c^* \Omega_c}{\delta_p - \delta_c} + \frac{\Omega_{c'}^* \Omega_{c'}}{\delta_p - \delta_{c'}} = 0. \quad (5)$$

In this case, the destructive quantum interference between the two excitation pathways ($|c\rangle$-$|a\rangle$ and $|c'\rangle$-$|a\rangle$) will cancel out the population that are from level $|c\rangle$ and level $|c'\rangle$ to the upper level $|a\rangle$. Therefore, a two-level dark state that consists of levels $|c\rangle$ and $|c'\rangle$ can be formed, and the four-level system will be reduced to a two-level system ($|a\rangle$, $|b\rangle$), namely, it seems that the two levels $|c\rangle$, $|c'\rangle$ as well as the two control fields Ω_c, $\Omega_{c'}$ are absent. In addition to the two-level dark state consisting of $|c\rangle$ and $|c'\rangle$, there is a three-level dark state formed by $|c\rangle$, $|c'\rangle$, and $|b\rangle$. In this case, the quantum-interference condition is given by

$$\Omega_c \rho_{cb} + \Omega_{c'} \rho_{c'b} + \Omega_p \rho_{bb} = 0. \quad (6)$$

With the help of this relation, one can show from the first formula in Eq. (1) that the steady density matrix element for $|a\rangle$-$|b\rangle$ coherence is $\rho_{ab} = 0$. Thus, the destructive quantum interference among the three excitation pathways, i.e., $|c\rangle$-$|a\rangle$, $|c'\rangle$-$|a\rangle$, and $|b\rangle$-$|a\rangle$, cancels out the population to the upper level $|a\rangle$ (from the three lower levels $|b\rangle$, $|c\rangle$, $|c'\rangle$). One can obtain a relation $(\Omega_c \rho_{cb} + \Omega_{c'} \rho_{c'b})/(\Omega_p \rho_{bb}) = -1$ from Eq. (6), and then the constructive quantum interference between the two transitions $|c\rangle$-$|a\rangle$ and $|c'\rangle$-$|a\rangle$ can be defined by using this relation. Although there is the destructive quantum interference occurring among the three transition pathways $|c\rangle$-$|a\rangle$, $|c'\rangle$-$|a\rangle$, and $|b\rangle$-$|a\rangle$, there is the constructive quantum interference between the two transition pathways $|c\rangle$-$|a\rangle$ and $|c'\rangle$-$|a\rangle$. In this case, the upper level $|a\rangle$ is empty (or the quantum coherence $\rho_{ab} = 0$), and the effect of electromagnetically induced transparency will be exhibited in the present four-level SQD medium.

Now we are in a position to obtain the explicit expression for the electric permittivity ε_1 of the quantum coherent (EIT) medium layer [see Fig. 1(a)]. Since the electric polarizability of the probe transition $|b\rangle$-$|a\rangle$ is $\varrho = 2\wp_{ba}\rho_{ab}/(\varepsilon_0 E_p) = 2|\wp_{ba}|^2 \rho_{ab}/(\varepsilon_0 \hbar \Omega_p)$, one can obtain $N\varrho$ as follows:

$$N\varrho = -\frac{N|\wp_{ab}|^2}{\varepsilon_0 \hbar} \frac{(\delta_p - \delta_c + i\gamma_{bc})(\delta_p - \delta_{c'} + i\gamma_{bc'})}{(\delta_p - \delta_c + i\gamma_{bc})(\delta_p - \delta_{c'} + i\gamma_{bc'})(\delta_p + i\gamma_{ab}) - \frac{1}{4}\Omega_c^* \Omega_c (\delta_p - \delta_{c'} + i\gamma_{bc'}) - \frac{1}{4}\Omega_{c'}^* \Omega_{c'} (\delta_p - \delta_c + i\gamma_{bc})}, \quad (7)$$

where N denotes the quantum-dot number density in the quantum coherent (EIT) medium. According to the Clausius-Mossotti relation that accounts for the contribution of all the other neighboring quantum dots (or microscopic structure units) to the polarization (local field correction), the relative electric permittivity of the EIT medium layer is given by $\varepsilon_1 = 1 + \frac{N\varrho}{1 - \frac{N\varrho}{3}}$. The electric permittivity of the four-level quantum coherent medium layer can have a negative real part and a large imaginary part (i.e., $|\mathrm{Re}\varepsilon_1| < \mathrm{Im}\varepsilon_1$) if the four-level system in Fig. 1(b) experiences *destructive* quantum interference between the $|c\rangle$-$|a\rangle$ and $|c'\rangle$-$|a\rangle$ transitions. However, the electric permittivity will have a large negative real part (i.e., $|\mathrm{Re}\varepsilon_1| \gg \mathrm{Im}\varepsilon_1$) if the *constructive* quantum interference between the $|c\rangle$-$|a\rangle$ and $|c'\rangle$-$|a\rangle$ transitions occurs. Then under certain proper conditions there will be surface plasmon wave excitation at the interface [at $x = 0$ in Fig. 1(a)] between the EIT layer with permittivity ε_1 and the bounding medium with permittivity ε_0. All these effects will be demonstrated in our numerical example.

B. An EIT-prism coupler

Now we shall present the theoretical mechanism of the EIT-prism coupler, including the optical response of the tunable reflection spectrum and the field distribution (determined by the boundary conditions on the two sides of the EIT layer) in the prism coupler. We assume the incidence plane is the $\hat{z}$-$\hat{x}$ plane. The magnetic field of a TM mode is $H_y(x,z) = H_y(x)e^{-i\beta z}$ (the convention of engineers for the phase factor [34,35] is adopted for the prism coupler). With the help of the Maxwell equations, the spatial distribution of the magnetic field in the prism coupler can be expressed as [16,36]

$$H_y(x) = \begin{cases} A_2 e^{\alpha_2(x-d)} + B_2 e^{-\alpha_2(x-d)}, & x > d \\ A_1 e^{\alpha_1 x} + B_1 e^{-\alpha_1 x}, & 0 < x < d \\ A_0 e^{\alpha_0 x}, & x < 0 \end{cases} \quad (8)$$

where $\alpha_j = (\beta^2 - k_0^2 \varepsilon_j^*)^{1/2}$ $(j = 0,1,2)$ and $\beta = k_0\sqrt{\varepsilon_2^*}\sin\theta$. Here, ε_j^* denotes the complex conjugate of ε_j because we have adopted the convention of engineers for the factor of phasor time dependence $e^{i\omega t}$ [34,35]. By substituting Eq. (8) into the electromagnetic boundary conditions [i.e., the tangential components of the electric and magnetic fields are, respectively, continuous at the interfaces at $x = 0$ and $x = d$ in Fig. 1(a)], we can obtain the magnetic field amplitudes. As the magnetic field is continuous across $x = 0$, we have $A_0 = A_1 + B_1$. The condition that the electric field is continuous means that $\frac{1}{\varepsilon^*}\frac{\partial H_y}{\partial x}$

is continuous across the interface. Thus, we have

$$\frac{\alpha_1}{\varepsilon_1^*}(A_1 - B_1) = \frac{\alpha_0}{\varepsilon_0}A_0. \tag{9}$$

Then we have the amplitudes of the magnetic field $H_y(x)$ in the thin layer of SQD medium,

$$A_1 = \frac{1}{2}A_0\left(1 + \frac{\varepsilon_1^*\alpha_0}{\varepsilon_0^*\alpha_1}\right), \quad B_1 = \frac{1}{2}A_0\left(1 - \frac{\varepsilon_1^*\alpha_0}{\varepsilon_0^*\alpha_1}\right). \tag{10}$$

For the interface at $x = d$, the boundary condition that the electric field and the magnetic field are, respectively, continuous leads to the relations,

$$\frac{\alpha_2}{\varepsilon_2^*}(A_2 - B_2) = \frac{\alpha_1}{\varepsilon_1^*}(A_1 e^{\alpha_1 d} - B_1 e^{-\alpha_1 d}),$$
$$A_2 + B_2 = A_1 e^{\alpha_1 d} + B_1 e^{-\alpha_1 d}. \tag{11}$$

Then the explicit expressions for A_2 and B_2 are given by

$$\begin{aligned} A_2 &= \frac{1}{2}\left[A_1 e^{\alpha_1 d}\left(1 + \frac{\varepsilon_2^*\alpha_1}{\varepsilon_1^*\alpha_2}\right) + B_1 e^{-\alpha_1 d}\left(1 - \frac{\varepsilon_2^*\alpha_1}{\varepsilon_1^*\alpha_2}\right)\right] \\ &= \frac{1}{4}A_0\left[e^{\alpha_1 d}\left(1 + \frac{\varepsilon_1^*\alpha_0}{\varepsilon_0^*\alpha_1}\right)\left(1 + \frac{\varepsilon_2^*\alpha_1}{\varepsilon_1^*\alpha_2}\right)\right. \\ &\quad \left. + e^{-\alpha_1 d}\left(1 - \frac{\varepsilon_1^*\alpha_0}{\varepsilon_0^*\alpha_1}\right)\left(1 - \frac{\varepsilon_2^*\alpha_1}{\varepsilon_1^*\alpha_2}\right)\right], \end{aligned} \tag{12}$$

$$\begin{aligned} B_2 &= \frac{1}{2}\left[A_1 e^{\alpha_1 d}\left(1 - \frac{\varepsilon_2^*\alpha_1}{\varepsilon_1^*\alpha_2}\right) + B_1 e^{-\alpha_1 d}\left(1 + \frac{\varepsilon_2^*\alpha_1}{\varepsilon_1^*\alpha_2}\right)\right] \\ &= \frac{1}{4}A_0\left[e^{\alpha_1 d}\left(1 + \frac{\varepsilon_1^*\alpha_0}{\varepsilon_0^*\alpha_1}\right)\left(1 - \frac{\varepsilon_2^*\alpha_1}{\varepsilon_1^*\alpha_2}\right)\right. \\ &\quad \left. + e^{-\alpha_1 d}\left(1 - \frac{\varepsilon_1^*\alpha_0}{\varepsilon_0^*\alpha_1}\right)\left(1 + \frac{\varepsilon_2^*\alpha_1}{\varepsilon_1^*\alpha_2}\right)\right]. \end{aligned} \tag{13}$$

The reflectance of an electromagnetic wave, e.g., a TM wave, is given by $R \equiv |B_2/A_2|^2$. Then one can have the explicit form of R,

$$R = \left|\frac{g_{12}\exp(+\alpha_1 d) + g_{01}\exp(-\alpha_1 d)}{\exp(+\alpha_1 d) + g_{12}g_{01}\exp(-\alpha_1 d)}\right|^2, \tag{14}$$

with $g_{01} = (\varepsilon_0^*\alpha_1 - \varepsilon_1^*\alpha_0)/(\varepsilon_0^*\alpha_1 + \varepsilon_1^*\alpha_0)$ and $g_{12} = (\varepsilon_1^*\alpha_2 - \varepsilon_2^*\alpha_1)/(\varepsilon_1^*\alpha_2 + \varepsilon_2^*\alpha_1)$. The electric field of the TM-mode surface plasmon wave can be expressed by

$$E_x(x) = \begin{cases} \frac{\beta}{\omega\varepsilon_2^*\varepsilon_0}(A_2 e^{\alpha_2(x-d)} + B_2 e^{-\alpha_2(x-d)}), & x > d, \\ \frac{\beta}{\omega\varepsilon_1^*\varepsilon_0}(A_1 e^{\alpha_1 x} + B_1 e^{-\alpha_1 x}), & 0 < x < d, \\ \frac{\beta}{\omega\varepsilon_0}\left(A_0 e^{\alpha_0 x}\right), & x < 0, \end{cases} \tag{15}$$

$$E_z(x) = \begin{cases} \frac{\alpha_2}{i\omega\varepsilon_2^*\varepsilon_0}(A_2 e^{\alpha_2(x-d)} - B_2 e^{-\alpha_2(x-d)}), & x > d \\ \frac{\alpha_1}{i\omega\varepsilon_1^*\varepsilon_0}(A_1 e^{\alpha_1 x} - B_1 e^{-\alpha_1 x}), & 0 < x < d \\ \frac{\alpha_0}{i\omega\varepsilon_0}\left(A_0 e^{\alpha_0 x}\right). & x < 0 \end{cases} \tag{16}$$

Now let us explain the concept of the surface-plasmon-polariton resonance for the present application: From Eq. (10), we have the magnetic field amplitude of the incident probe wave in the layer $A_1 = \frac{1}{2}A_0(1 + \frac{\varepsilon_1^*\alpha_0}{\varepsilon_0^*\alpha_1})$. If the layer thickness d is adequately large, then the condition $1 + \frac{\varepsilon_1^*\alpha_0}{\varepsilon_0^*\alpha_1} \to 0$ will be fulfilled for the surface plasmon wave excitation on a single flat interface (at $x = 0$) [16,17]. Thus, in order to have a finite amplitude A_1, this requires that the surface plasmon wave amplitude A_0 (on the interface at $x = 0$) needs to be divergent. Such a phenomenon can be referred to as "surface-plasmon-polariton resonance."

In the present EIT-prism coupling system, the thickness of the EIT medium layer $d = 50$ nm, the relative electric permittivity of the prism dielectric $\varepsilon_2 = 3.24$, and the wavelength of the incident light in vacuum is $\lambda = 632.8$ nm [19,36]. The typical parameters of the four-level system are chosen as follows: The spontaneous emission decay rate $\gamma_{ab} = 1.0 \times 10^{10}\text{s}^{-1}$ [37,38], the collisional dephasing rates $\gamma_{bc} = \gamma_{ab}/50$, $\gamma_{bc'} = \gamma_{ab}/25$ [39], the electric dipole moment $\wp_{ab} = 6.3 \times 10^{-28}\text{C m}$ [37,40], the Rabi frequency of one of the control field $\Omega_{c'} = 6.0\gamma_{ab}$, the detuning frequencies $\delta_{c'} = -0.4\gamma_{ab}$, $\delta_c = 1.2\gamma_{ab}$, and the EIT layer density $N = 1.0 \times 10^{21}$ m^{-3} [37,41]. These parameters will be adopted throughout this work.

III. THE REFLECTION SPECTRUM OF THE EIT-PRISM COUPLER

In the preceding section, we have shown that the $|b\rangle$-$|a\rangle$ transition (driven by the probe wave A_2) can be manipulated via the destructive or constructive quantum interference between the $|c\rangle$-$|a\rangle$ and $|c'\rangle$-$|a\rangle$ transitions. If the destructive quantum interference between the $|c\rangle$-$|a\rangle$ and $|c'\rangle$-$|a\rangle$ transitions occurs, the two levels $|c\rangle$ and $|c'\rangle$ seem to be absent, and then the four-level system $\{|a\rangle,|b\rangle,|c\rangle,|c'\rangle\}$ will be equivalent to a two-level one $\{|a\rangle,|b\rangle\}$. This will give rise to an effect of two-level resonant absorption. Thus, the destructive interference (between $|c\rangle$-$|a\rangle$ and $|c'\rangle$-$|a\rangle$ transition pathways) makes the four-level medium lossy, i.e., the imaginary part of the electric permittivity ε_1 of the thin EIT layer will be large, and the surface-plasmon-polariton resonance will be inhibited (or the excited surface plasmon polaritons will be dissipated drastically). But in the case of the constructive quantum interference between $|c\rangle$-$|a\rangle$ and $|c'\rangle$-$|a\rangle$ transitions, such resonant absorption does not occur (i.e., the imaginary part of the electric permittivity ε_1 of the thin layer is relatively small), and hence the surface plasmon polaritons can be excited relatively easily.

Now we will consider the tunable reflection spectrum of the EIT-prism coupler. This reflection spectrum will depend critically on some parameters of the four-level system in the thin layer (such as the frequency detuning and the Rabi frequencies of the control fields). The electric permittivity of the EIT layer depending upon the frequency detuning δ_p of the incident probe light and the Rabi frequency Ω_c of the control field (driving the $|c\rangle$-$|a\rangle$ transition) are presented in Figs. 2–4, where two typical cases (*destructive* quantum interference between $|c\rangle$-$|a\rangle$ and $|c'\rangle$-$|a\rangle$ transitions when the Rabi frequency $\Omega_c = \Omega_{c'}$, and *constructive* quantum interference between $|c\rangle$-$|a\rangle$ and $|c'\rangle$-$|a\rangle$ transitions when the Rabi frequency $\Omega_c = \Omega_{c'}/5$) are illustrated as an example. In what follows, we shall interpret why we choose these two

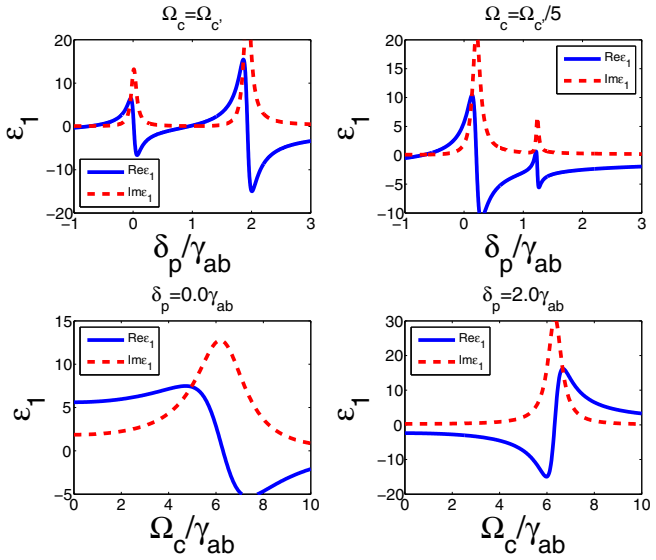

FIG. 2. (Color online) The real and imaginary parts of the electric permittivity of the EIT layer depending upon the frequency detuning δ_p of the incident probe light and the Rabi frequency Ω_c of the control field. $\Omega_c = \Omega_{c'}$ ($\Omega_c = \Omega_{c'}/5$) corresponds to the case of destructive (constructive) quantum interference between $|c\rangle$-$|a\rangle$ and $|c'\rangle$-$|a\rangle$ transitions.

values for the Rabi frequencies of the two external control fields.

It can be found from Eqs. (4) and (5) that when the *interference term* in the square brackets, i.e., $\frac{\Omega_c^*\Omega_c}{\delta_p-\delta_c} + \frac{\Omega_{c'}^*\Omega_{c'}}{\delta_p-\delta_{c'}}$ vanishes (or becomes quite small), we can say that there is destructive interference in the level transition process (between $|c\rangle$-$|a\rangle$ and $|c'\rangle$-$|a\rangle$ transitions), while when the interference term $\frac{\Omega_c^*\Omega_c}{\delta_p-\delta_c} + \frac{\Omega_{c'}^*\Omega_{c'}}{\delta_p-\delta_{c'}}$ is quite large (e.g., it has the order of magnitude of the Rabi frequency Ω_c), we can say that there is constructive interference between $|c\rangle$-$|a\rangle$ and $|c'\rangle$-$|a\rangle$ transitions. From this definition, for the frequency detuning

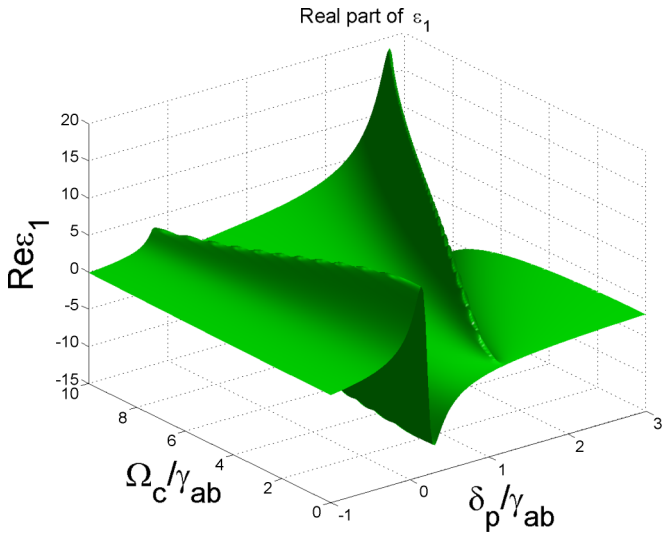

FIG. 3. (Color online) The tunable behavior of dispersion in the real part of the electric permittivity of the EIT medium layer.

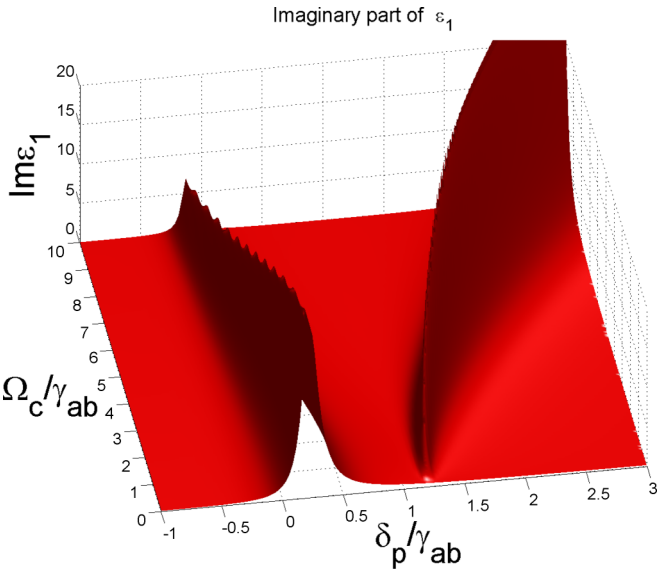

FIG. 4. (Color online) The tunable behavior of dispersion in the imaginary part of the electric permittivity of the EIT medium layer.

range of δ_p of interest, we can have the result that when the two Rabi frequencies, Ω_c and $\Omega_{c'}$, of the control fields are close ($\Omega_c \simeq \Omega_{c'}$), it will lead to the destructive interference. In the numerical example, we choose $\Omega_c = \Omega_{c'}$. However, when one of the two Rabi frequencies is much smaller than the other, it will lead to the constructive interference. In the paper, we choose $\Omega_c = \Omega_{c'}/5$ as an illustrative example for the constructive interference.

It has been shown in Figs. 2 and 3 that, under certain proper conditions, the electric permittivity of the EIT layer can have a negative real part, which can support the existence of the surface plasmon wave. The reflection spectrum depending upon the angle of incidence θ of the probe field on the prism base is presented in Fig. 5, where the two representative cases, i.e., double-control destructive quantum interference (e.g., $\Omega_c = \Omega_{c'}$) and double-control constructive interference (e.g., $\Omega_c = \Omega_{c'}/5$) have been considered. The wave vector of the incident probe field in the $\hat{z}$ direction (parallel to the prism base) in this EIT-prism coupler can be equal to the phase constant of surface plasmon wave if we tune the angle of incidence of the probe field on the prism base (at $x = d$). Such a surface plasmon wave mode can then be excited at the interface (at $x = 0$) if we choose a proper thickness d of the EIT medium layer whose permittivity is ε_1 [see Fig. 1(a)]. This means that the EIT-prism system couples the incident probe wave into the surface plasmon wave mode. As a result, the reflectance at the prism-EIT interface (i.e., the prism base at $x = d$) decreases dramatically. In the case of double-control constructive interference (i.e., $\Omega_c = \Omega_{c'}/5$), in which the permittivity ε_1 of the quantum coherent medium layer can exhibit some of the metal characteristics, e.g., ε_1 has a large negative real part and a relatively small imaginary part [if δ_p is close to $\delta_{c'}$, then the imaginary part of the permittivity ε_1 would be quite small because of the two-photon resonance and dark-state population trapping ($|b\rangle$ and $|c'\rangle$ form a dark state)], the reflectance R increases to 0.9 (close to the value of R in total internal reflection) when the angle of

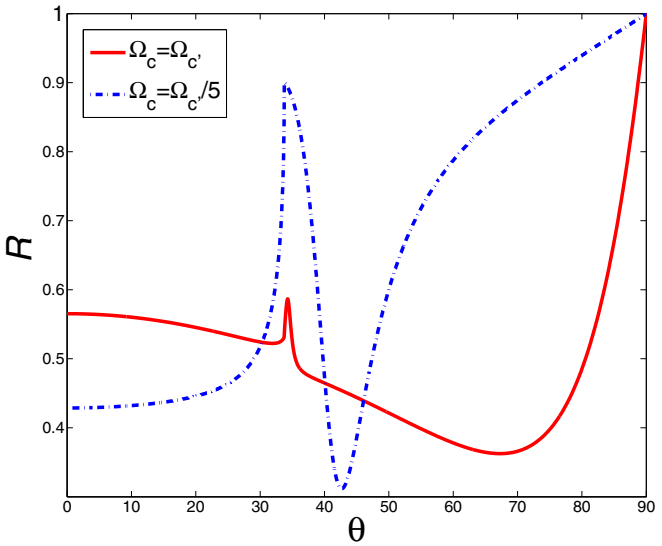

FIG. 5. (Color online) The tunable reflection spectrum (i.e., the dimensionless reflectance R depending on the incidence angle θ) due to destructive ($\Omega_c = \Omega_{c'}$) and constructive ($\Omega_c = \Omega_{c'}/5$) quantum interference in the EIT-prism coupling system. The unit of the incidence angle θ is degree (°). The detuning frequencies of the three optical fields are chosen as $\delta_p = 2.0\gamma_{ab}$, $\delta_{c'} = -0.4\gamma_{ab}$, and $\delta_c = 1.2\gamma_{ab}$. The switchable permittivity ε_1 of the quantum coherent (EIT) medium layer is $-14.9 + 16.5i$ (when $\Omega_c = \Omega_{c'}$ for destructive quantum interference) and $-2.52 + 0.31i$ (when $\Omega_c = \Omega_{c'}/5$ for constructive quantum interference).

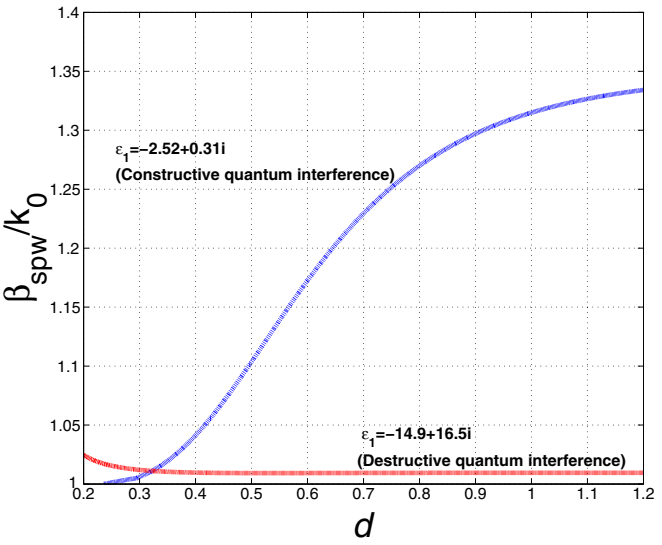

FIG. 6. (Color online) The phase constant $\beta_{\rm spw}$ of the surface plasmon polaritons excited on the EIT layer surface corresponding to the two cases of destructive and constructive quantum interference between $|c\rangle$-$|a\rangle$ and $|c'\rangle$-$|a\rangle$ transitions. The parameter for normalizing the phase constant $\beta_{\rm spw}$ is $k_0 = \omega/c$ with ω the probe frequency $\omega_{\rm p}$. The variable d denotes the EIT layer thickness (in units of c/ω).

incidence θ at the prism-EIT interface (at $x = d$) becomes large. Then when $\theta > 35$ degrees, R will, however, drop to a small value, e.g., $R \simeq 0.3$ at $\theta \simeq 43$ degrees. This is an attenuated total reflection (ATR) effect, since the surface-plasmon-polariton excitation occurs at the lower surface (at $x = 0$) of the quantum coherent (EIT) medium layer, and the incident probe light has been coupled into this thin EIT layer as a surface plasmon wave mode. For the case of destructive quantum interference (i.e., $\Omega_{\rm c} = \Omega_{\rm c'}$) between the $|c\rangle$-$|a\rangle$ and $|c'\rangle$-$|a\rangle$ transitions, such an ATR effect arises at large angle of incidence, e.g., R decreases to its minimum at $\theta \simeq 67$ degrees, and then begins to increase to 1 when $\theta > 67$ degrees. However, the surface-plasmon-polariton resonance in the case of destructive quantum interference is not significant because of the high loss in the quantum coherent medium layer. Therefore, we shall concentrate our attention on the case of constructive quantum interference (the significant process of surface-plasmon-polariton excitation will be addressed in the next section).

IV. THE QUANTUM-INTERFERENCE SWITCHABLE REFLECTION SPECTRUM AND THE OPTICAL EXCITATION OF THE SURFACE WAVE

In order to treat the optical excitation of the surface wave, the phase constant (real part) $\beta_{\rm spw}$ of the surface plasmon wave on the EIT layer surface is given in Fig. 6. Here, the phase constant is the solution of the equation of dispersion relation (to be given below). By following the theoretical treatment of the thin film surface optics [17,36], the dispersion relation of the present EIT layer structure is given by

$$e^{-2\alpha_1 d} = \left(\frac{1+\frac{\alpha_0\varepsilon_1^*}{\alpha_1\varepsilon_0}}{1-\frac{\alpha_2\varepsilon_1^*}{\alpha_1\varepsilon_2^*}}\right)\left(\frac{1+\frac{\alpha_2\varepsilon_1^*}{\alpha_1\varepsilon_2^*}}{1-\frac{\alpha_0\varepsilon_1^*}{\alpha_1\varepsilon_0}}\right), \tag{17}$$

where the attenuation coefficients are defined as $\alpha_j = \sqrt{\beta_{\rm spw}^2 - \varepsilon_j^*(\omega/c)^2}$ $(j = 0,1,2)$. In the case of destructive quantum interference between $|c\rangle$-$|a\rangle$ and $|c'\rangle$-$|a\rangle$ transitions, the absorptive loss in the EIT layer is high, and the surface plasmon wave is difficult to be generated (besides, phase matching, including momentum conservation in the direction of interface, cannot be preserved). In the case of constructive quantum interference, however, the loss is relatively small, and the surface plasmon wave can be relatively easy to be excited.

In what follows, for Figs. 7–10, we shall study only the SPPs excited by an incident probe wave at a particular frequency, i.e., $\omega_p = \omega_{ab} + \delta_p$ with the frequency detuning $\delta_p = 2.0\gamma_{ab}$. For this probe frequency, the permittivity ϵ_1 of the thin layer has a definite value ($\varepsilon_1 = -2.52 + 0.31i$).

Now we are in a position to consider the problem of optical excitation of the surface waves in this prism coupler. It can be seen in Fig. 7 that there is a transmitted wave from the SQD medium layer into vacuum (at $x < 0$) when the angle of incidence $\theta = 30$ degrees, and the wave is almost totally reflected (e.g., the reflectance $R \simeq 0.9$ at the prim base) when $\theta = 35$ degrees. When the angle of incidence $\theta = 40 \sim 45$ degrees, however, the surface-plasmon-polariton resonance occurs, and hence the surface plasmon wave is excited at the interface ($x = 0$ plane between vacuum and the quantum-coherent medium layer) by the incident wave. This corresponds to the constructive quantum interference between the $|c\rangle$-$|a\rangle$ and $|c'\rangle$-$|a\rangle$ transitions (with $\Omega_c = \Omega_{c'}/5$). As a

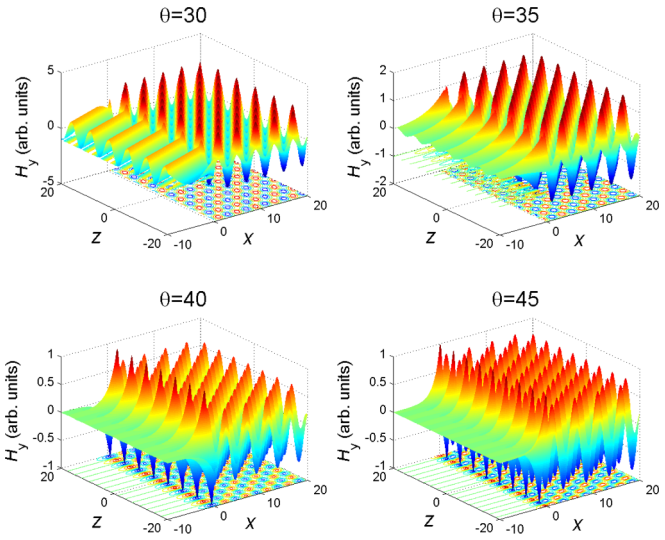

FIG. 7. (Color online) The spatial profile of the magnetic field H_y of the TM wave in the prism coupler corresponding to $\varepsilon_1 = -2.52 + 0.31i$ (i.e., constructive quantum interference with $\Omega_c = \Omega_{c'}/5$). The x and z are the coordinate axes (in units of c/ω) that are normal and parallel, respectively, to the flat surface of the EIT layer in the present prism coupler (seen in Fig. 1). When the angle of incidence θ is $40 \sim 45$ degrees, the amplitude of the excited surface wave at the plane of $x = 0$ will be larger than that of the incident (illuminating) light (propagating in the region of $x > 0$), which excites the surface wave at $x = 0$.

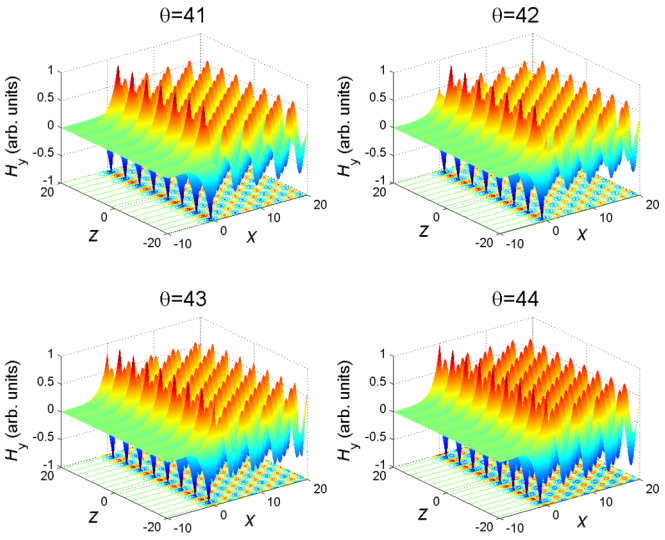

FIG. 8. (Color online) Optical excitation of the magnetic field H_y of the surface plasmon wave (in the region of $x \leqslant 0$) corresponding to the case of constructive quantum interference. The x and z are the coordinate axes (in units of c/ω) that are normal and parallel, respectively, to the flat surface of the EIT layer in the present prism coupler (seen in Fig. 1). The angle of incidence of the probe light is $\theta = 41$–44 degrees. The amplitude of the excited surface plasmon wave (at the plane of $x = 0$) is larger than that of the incident probe light (in the region of $x > 0$).

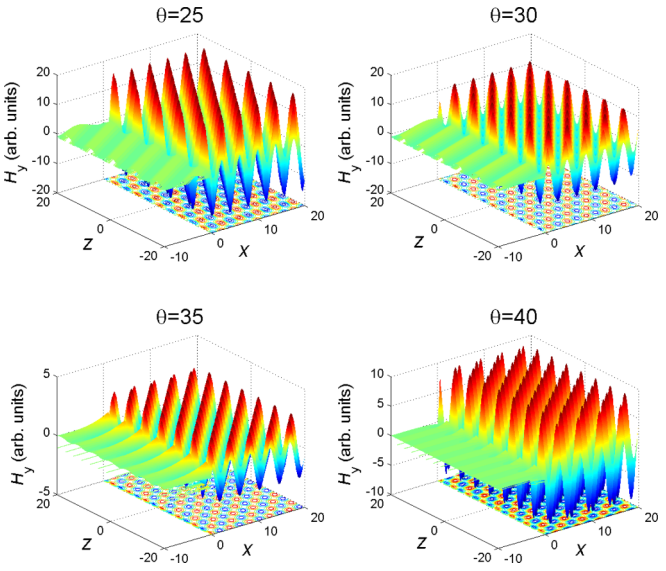

FIG. 9. (Color online) The spatial profile of the magnetic field H_y of the TM wave in the prism coupler corresponding to $\varepsilon_1 = -14.9 + 16.5i$ (i.e., destructive quantum interference with $\Omega_c = \Omega_{c'}$). The x and z are the coordinate axes (in units of c/ω) in the present prism coupler.

result, the reflectance R drops to a small number (attenuated total reflection when $35 < \theta < 40$ degrees).

The wave vector dependence can be exhibited by the incidence angle θ (of the probe light). In the following figures, the incidence angle θ is tunable, and it will provide an appropriate β that triggers the excitation. For example, in Fig. 8, it can be seen that when the incidence angle $\theta = 43^\circ$, the surface plasmon polaritons can be excited (i.e., at the interface $x = 0$, the amplitude is larger than that of the illuminating light). In order to manifest the evanescent feature of the surface wave more clearly, the spatial profile of the magnetic field H_y of the excited surface plasmon wave is presented in Fig. 8. As we have seen, in the tunable reflection spectrum of Fig. 5, the reflectance R (in the case of constructive quantum interference) decreases to its minimum and the attenuated total internal reflection occurs when the angle of incidence θ of the illuminating probe light is about 42–43 degrees. This means that the projection value (vector component) β $(=\sqrt{\varepsilon_2}(\omega/c)\sin\theta)$ of the wave vector of the incident probe light (illuminating the EIT layer through the prism) in the $\hat{z}$ direction parallel to the EIT layer surface is equal to the phase constant $\beta_{\rm spw}$ obtained in the dispersion relation (17), and hence the surface plasmon wave is excited. It should be emphasized that when the surface plasmon wave (in the region of $x \leqslant 0$) is excited (shown in Fig. 8), its amplitude (at the plane of $x = 0$) is twice that of the incident probe light (illuminating the EIT layer through the prism in the region of $x > 0$). The fact that *the amplitude excited at the interface $x = 0$ is larger than that of the illuminating light* can be identified as a visual criterion for the surface plasmon wave excitation.

We shall, on the other hand, interpret the evanescent feature of the surface wave with the help of the attenuation coefficients. One can see from Fig. 6 that the phase constant $\beta_{\rm spw}$ of the

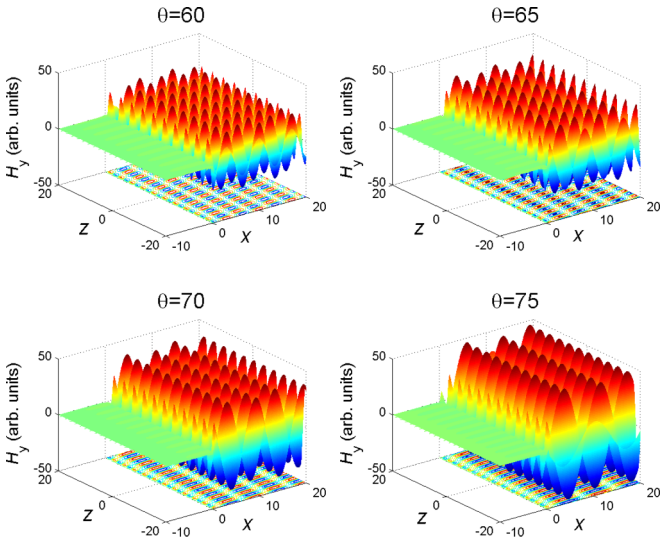

FIG. 10. (Color online) The spatial profile of the magnetic field H_y of the TM wave in the prism coupler corresponding to $\varepsilon_1 = -14.9 + 16.5i$ (i.e., destructive quantum interference with $\Omega_c = \Omega_{c'}$). The x and z are the coordinate axes (in units of c/ω) in the present prism coupler.

surface plasmon wave excited in the present prism coupler is $1.1\omega/c$ when the EIT layer thickness $d = 50$ nm (in the case of constructive quantum interference). Then from the relation $\alpha_j = \sqrt{\beta_{\rm spw}^2 - \varepsilon_j^*(\omega/c)^2}$ $(j = 0,1,2)$, the "attenuation coefficients" are given by $\alpha_0 = 0.46\omega/c$ (in the vacuum substrate in the region of $x < 0$), $\alpha_1 = (1.9 - 8.0 \times 10^{-2}i)\omega/c$ (in the EIT layer, $0 < x < 50$ nm), and $\alpha_2 = (0.0 + 1.4i)\omega/c$ (in the prism in the region of $x > 50$ nm). Since the attenuation coefficient in the vacuum substrate (under the interface of the EIT layer) is a real number ($\alpha_0 = 0.46\omega/c$), the surface plasmon wave excited by the illuminating light will decay exponentially (in the region of $x < 0$) with increasing distance from the $x = 0$ interface. The attenuation length is $1/\alpha_0 = 2.2c/\omega$, i.e., the surface wave in vacuum is strongly confined to the interface $x = 0$ between vacuum and the quantum-coherent medium layer.

For comparison, we shall consider briefly the destructive quantum interference. According to the reflection spectrum shown in Fig. 5, there are two ranges of θ, which are of particular interest to us: [25,40] degrees (the reflectance R increases to its local maximum corresponding to the "total" internal reflection) and [60,75] degrees (the reflectance R decreases to its minimum corresponding to the attenuated total reflection due to the surface plasmon wave excitation). But we should point out that the reflectance R (corresponding to the "total" internal reflection) cannot approach 1 because of the high loss in the SQD layer, and the effect of attenuated total reflection in the incidence angle range [60,75] degrees is not obvious, either (also because of the high loss). We plot the spatial field profile of the wave for the two incidence angle ranges, [25,40] degrees (in Fig. 9) and [60,75] degrees (in Fig. 10). In this case, the SQD medium layer is quite lossy (because of the destructive quantum interference between the two transitions driven by the two control fields) in the case of Figs. 9 and 10, and so the reflectance R (see Fig. 5) on the prism base is relatively small (e.g., $R < 0.6$). But there is still a minor peak of the reflectance at $\theta = 35$ degrees corresponding to the total reflection. Then it follows from Fig. 9 that there is a transmitted wave of small intensity when $\theta < 35$ degrees, and when $\theta > 35$ degrees, the surface plasmon wave should have been excited. However, the surface wave amplitude at the interface of $x = 0$ is small (or negligibly small) compared with the amplitude of the illuminating light (incident from the region of $x > 0$), as shown in Fig. 10. The surface plasmon wave cannot be excited (or excited but suppressed immediately) because of the high loss in the SQD layer (in the case of destructive quantum interference between the $|c\rangle$-$|a\rangle$ and $|c'\rangle$-$|a\rangle$ transitions).

V. DISCUSSIONS OF CHARACTERISTICS OF THE EIT-BASED SURFACE-PLASMON-POLARITON RESONANCE

We have addressed the condition of EIT-based surface-plasmon-polariton resonance. Obviously, it will be more difficult in displaying such quantum-dot sustained SPPs than in displaying the conventional metal-sustained SPPs. But it is still worth considering the possibility of *surface-plasmon-polariton resonance* and *quantum-dot sustained SPPs* based on the previous references for "quantum-dot plasmonics" [30–32]. The present scheme for exciting SPPs with controlled quantum coherence requires a quantum-dot medium layer with 20–120 nm in thickness [shown in Fig. 1(a) in the paper]. The techniques for multilayer self-assembled quantum dots (and for dielectric slabs doped or coated with quantum dots) have been developed [28,42,43]. Such quantum-dot films can be utilized in the present scenario. The quantum-dot thin medium layer would have a *negative* permittivity in certain probe frequency ranges, as shown in Fig. 2, by tuning the Rabi frequencies (and choosing its proper values) for the external control fields. The possibility of such a *negative* permittivity in a quantum-dot material has also been considered by other authors [44]. Therefore, according to the model and numerical calculation in the paper, it is possible for the SPPs excited on the quantum-dot medium layer in the present scenario. In order to support this possibility, we shall give evidence that is relevant to the present *quantum-dot sustained SPPs*: experimental demonstration of surface plasmon resonance in doped semiconductor quantum dots [30–32,45]. In the literature, such studies extend the conventional metal nanoplasmonics to a new area "quantum-dot plasmonics" (for example, the self-doped copper chalcogenides and metal oxides used in this new field of plasmonics are called the "plasmonic quantum dots") [45–47]. Thus, we expect that the surface-plasmon-polariton resonance and excitation with quantum-dot materials could in principle be exhibited based on the current technology [28,30–32,42,43,45].

We shall point out that the EIT-based surface-plasmon-polariton resonance presented in this paper has some attractive characteristics: (i) switchable quantum interference exhibited by surface plasmon wave excitation, (ii) coherently controllable surface plasmon wave by external optical fields, (iii) surface wave sensitive to dispersion of the SQD quantum coherent medium. The first two features have been shown in the preceding sections. Now we will address the third feature.

It should be noted that the conventional surface plasmon waves were generated (excited) at the interface between a dielectric and a metal [36]. The relative permittivity, $\varepsilon_m = 1 - \omega_p^2/\omega^2$, of a metal is not quite sensitive to the frequency, since the variable (frequency) appears as $1/\omega^2$ in the permittivity. Since a semiconductor-quantum-dot system driven by a light field is governed by quantum mechanics, in which the Schrödinger equation is a first order differential equation of time, the frequency will appear as $1/\delta$ with the frequency detuning $\delta = \omega - \omega_{ab}$, where ω_{ab} denotes the level transition frequency and ω the mode frequency of the incident light. Therefore, the dispersion in the permittivity of the SQD medium is quite strong, e.g., 10^5 times that in metal. This can be interpreted in more details as follows: In general, the relative permittivity of an SQD medium is $\varepsilon_s = 1 + \omega_0/(\omega_{ab} - \omega)$ (for convenience, we choose a simple two-level system as an illustrative example), where $\omega_0 = N|\wp_{ab}|^2/(\varepsilon_0\hbar)$ with N, $\wp_{ab}$, ε_0, and $\hbar$ the SQD number density, the electric-transition dipole moment, the vacuum permittivity, and the Planck constant, respectively. Here, we have assumed the imaginary part of ε_s is negligibly small. Note that the dispersion of a permittivity ε can be characterized by $d\varepsilon/d\omega$. Then it can be readily verified that the dispersion of ε_m (a metal) and ε_s (an SQD quantum coherent medium) is of the form,

$$\frac{d\varepsilon_m}{d\omega} = \left(2\frac{\omega_p^2}{\omega^2}\right)\frac{1}{\omega},$$
$$\frac{d\varepsilon_s}{d\omega} = \left(\frac{\omega_0}{\omega - \omega_{ab}}\right)\frac{1}{\omega - \omega_{ab}}. \tag{18}$$

It should be noted that the terms in the parentheses have the same (or almost the same) order of magnitude. In general, for a metal-substrate prism coupler, the typical value of the frequency of the incident light for surface plasmon wave excitation is $\omega = 10^{15} \sim 10^{16}$ s^{-1}, and in an ordinary experiment of quantum-coherent SQD dielectrics (on the topics of SQD phase coherence) [37,38], the frequency detuning $|\omega - \omega_{ab}|$ of an applied beam is about $10^{10} \sim 10^{11}$ s^{-1}. Thus, the ratio of dispersion in Eq. (18) at a certain frequency ($\omega = 10^{15} \sim 10^{16}$ s^{-1}) is given by

$$\left|\frac{\frac{d\varepsilon_s}{d\omega}}{\frac{d\varepsilon_m}{d\omega}}\right| \simeq 10^5. \tag{19}$$

This, therefore, means that, if it is excited in the present EIT-based prism coupler, the surface wave would be more dispersion sensitive than that in the conventional metal-based prism coupler. If, for example, the frequency of the incident light changes at only the level of one part in 10^5, the reflectance in the present EIT-based prism coupler will change dramatically. In contrast, the reflectance in the metal-based prism coupler does not change at all (or only a little change in the reflectance) if the frequency of the incident light changes at only the level of one part in 10^5. For this reason, we suggest that the dispersion-sensitive EIT-based prism coupler, which also seems to be an experimentally feasible scheme for exciting surface wave, deserves further consideration in the practical applications.

In the present paper, we have addressed the influence of SQD quantum coherence on the surface-plasmon-polariton excitation. But it should be pointed out that such an EIT-prism system can also make use of a prism with a four-level EIT atomic vapor cell bounding its prism base. The four-level system $\{|b\rangle,|c\rangle,|c'\rangle,|a\rangle\}$ [see Fig. 1(b) for its energy level configuration] interacts with three laser beams, i.e., the two control fields and one probe field couple the level pairs $|c\rangle$-$|a\rangle$, $|c'\rangle$-$|a\rangle$, and $|b\rangle$-$|a\rangle$, respectively. The four-level atomic system $\{|b\rangle,|c\rangle,|c'\rangle,|a\rangle\}$ in Fig. 1(b) can be found in neutral alkali-metal atoms, e.g., the neutral sodium atomic system $\{3^2S_{\frac{1}{2}},4^2S_{\frac{1}{2}},3^2D_{\frac{3}{2}},4^2P_{\frac{1}{2}}\}$ with the energy levels $\{0.000,25739.991,29172.889,30266.99\}\text{cm}^{-1}$ [48] and the neutral rubidium atomic system $\{5^2S_{\frac{1}{2}},4^2D_{\frac{3}{2}},6^2S_{\frac{1}{2}},6^2P_{\frac{1}{2}}\}$ with the energy levels $\{0.000,19355.649,20132.510,23715.081\}$ cm^{-1} [49]. For an atomic EIT-prism coupler with the atomic vapor cell adjacent to the prism base, the dispersion sensitivity of surface-plasmon-polariton resonance and excitation (in such a *plasmonic atomic vapor*) will be more significant, e.g., the ratio $|\frac{\frac{d\varepsilon_s}{d\omega}}{\frac{d\varepsilon_m}{d\omega}}|$ (dispersion sensitivity) defined in (19) will increase to the order 10^8.

VI. CONCLUDING REMARKS

An EIT-prism coupler has been suggested to realize tunable reflection spectrum with a mechanism of quantum-coherently controllable surface-plasmon-polariton excitation via *destructive* and *constructive* quantum interference that occurs among multilevel transition pathways driven by external control fields. The surface plasmon excitation modes, which are produced by coupling an incident probe field into a quantum coherent (EIT) medium layer, can be coherently manipulated through switchable quantum interference if we tune the intensity ratio of two control fields, which drive a four-level quantum coherent system. Some new photonic devices (e.g., logic and functional gates, where the two applied control fields act as input signals) and sensitively switchable devices (for, e.g., photonic microcircuits) could be designed by taking advantage of this quantum-interference switchable ATR effect accompanied by surface-plasmon-polariton resonance.

We must emphasize why we expect to employ quantum-dot media in sustaining SPPs: The advantage of quantum-dot sustained SPPs is that the SPPs are extremely frequency sensitive [the dispersion in quantum-dot dielectric is a few (e.g., five) orders of magnitude larger than that in metal, i.e., $|\frac{\frac{d\varepsilon_{\text{QD}}}{d\omega}}{\frac{d\varepsilon_{\text{metal}}}{d\omega}}| \simeq 10^5$). Clearly, this is also the physical origin of slow light by means of quantum dots [40,50,51].

In the literature, there have been some ideas of all-optical switching with quantum coherence in atomic vapor as well as classical EIT effect in on-chip optical resonator systems [52–54]. The present scheme (*tunable surface-plasmon-polariton resonance through switchable quantum interference in an EIT-prism coupler*) could also have such applications. In this paper, the quantum coherence (two-control EIT) is employed for realizing a tunable reflection spectrum of a probe field on the prism base (coupled to an EIT quantum coherent medium). Since *destructive* quantum interference between two transitions (i.e., $|c\rangle$-$|a\rangle$ and $|c'\rangle$-$|a\rangle$ transitions driven by the two control fields) can be switched to *constructive* quantum interference and vice versa (only by

changing the intensity ratio of the two control fields), such a controllable optical response based on quantum-interference switchable surface-plasmon-polariton resonance in the present EIT-prism coupling system may also be utilized to design photonic devices that could be used to realize the effect of all-optical switching. By tuning the intensities (or the intensity ratio) of the applied control fields, the EIT-prism coupler would enable us to achieve some applications of optical processing through *switchable quantum interference* and *tunable surface-plasmon-polariton resonance*. Since the surface plasmon (polariton) resonance, which can be dynamically tuned (based on switchable quantum interference through manipulating external control fields) in quantum dots, would have potential applications for technology of light propagation control and information processing, we hope it would be realized experimentally in the near future.

ACKNOWLEDGMENTS

This work is supported in part by the National Natural Science Foundation of China under Grants No. 11174250, No. 91233119, and No. 60990320, and by the Program of Zhejiang Leading Team of Science and Technology Innovation.

APPENDIX: THE EQUATION OF MOTION OF THE DENSITY MATRIX

We shall present the equation of motion of the density matrix of the double-control four-level system. This system interacts with three optical fields, i.e., the two control laser beams and one probe laser beam, which couple the level pairs $|c\rangle$-$|a\rangle$, $|c'\rangle$-$|a\rangle$, and $|b\rangle$-$|a\rangle$, respectively [see Fig. 1(b)]. According to the Schrödinger equation, the equations of the density matrix elements are given by

$$i\frac{\partial\rho_{aa}}{\partial t} = -i(\Gamma_{ac'}+\Gamma_{ab}+\Gamma_{ac})\rho_{aa} + \left(\frac{\Omega_p^*}{2}\rho_{ab} + \frac{\Omega_c^*}{2}\rho_{ac} + \frac{\Omega_{c'}^*}{2}\rho_{ac'}\right) - \left(\frac{\Omega_p}{2}\rho_{ba} + \frac{\Omega_c}{2}\rho_{ca} + \frac{\Omega_{c'}}{2}\rho_{c'a}\right), \tag{A1a}$$

$$i\frac{\partial\rho_{bb}}{\partial t} = i(\Gamma_{ab}\rho_{aa} + \Gamma_{c'b}\rho_{c'c'} + \Gamma_{cb}\rho_{cc}) + \frac{\Omega_p}{2}\rho_{ba} - \frac{\Omega_p^*}{2}\rho_{ab}, \tag{A1b}$$

$$i\frac{\partial\rho_{cc}}{\partial t} = i(\Gamma_{ac}\rho_{aa} + \Gamma_{c'c}\rho_{c'c'} - \Gamma_{cb}\rho_{cc}) + \frac{\Omega_c}{2}\rho_{ca} - \frac{\Omega_c^*}{2}\rho_{ac}, \tag{A1c}$$

$$i\frac{\partial\rho_{c'c'}}{\partial t} = i\left[\Gamma_{ac'}\rho_{aa} - \left(\Gamma_{c'c}+\Gamma_{c'b}\right)\rho_{c'c'}\right] + \frac{\Omega_{c'}}{2}\rho_{c'a} - \frac{\Omega_{c'}^*}{2}\rho_{ac'}, \tag{A1d}$$

$$i\frac{\partial\rho_{ab}}{\partial t} = \left[-i\left(\frac{\Gamma_{ac'}+\Gamma_{ab}+\Gamma_{ac}}{2} + \Gamma_{ab}^{(\mathrm{ph})}\right) - \delta_p\right]\rho_{ab} + \frac{\Omega_p}{2}\rho_{aa} - \left(\frac{\Omega_p}{2}\rho_{bb} + \frac{\Omega_c}{2}\rho_{cb} + \frac{\Omega_{c'}}{2}\rho_{c'b}\right), \tag{A1e}$$

$$i\frac{\partial\rho_{ac}}{\partial t} = \left[-i\left(\frac{\Gamma_{ac'}+\Gamma_{ab}+\Gamma_{ac}+\Gamma_{cb}}{2} + \Gamma_{ac}^{(\mathrm{ph})}\right) - \delta_c\right]\rho_{ac} + \frac{\Omega_c}{2}\rho_{aa} - \left(\frac{\Omega_p}{2}\rho_{bc} + \frac{\Omega_c}{2}\rho_{cc} + \frac{\Omega_{c'}}{2}\rho_{c'c}\right), \tag{A1f}$$

$$i\frac{\partial\rho_{ac'}}{\partial t} = \left[-i\left(\frac{\Gamma_{ac'}+\Gamma_{ab}+\Gamma_{ac}+\Gamma_{c'c}+\Gamma_{c'b}}{2} + \Gamma_{ac'}^{(\mathrm{ph})}\right) - \delta_{c'}\right]\rho_{ac'} + \frac{\Omega_{c'}}{2}\rho_{aa} - \left(\frac{\Omega_p}{2}\rho_{bc'} + \frac{\Omega_c}{2}\rho_{cc'} + \frac{\Omega_{c'}}{2}\rho_{c'c'}\right), \tag{A1g}$$

$$i\frac{\partial\rho_{bc}}{\partial t} = \left[-i\left(\frac{\Gamma_{cb}}{2} + \Gamma_{bc}^{(\mathrm{ph})}\right) + (\delta_p - \delta_c)\right]\rho_{bc} + \frac{\Omega_c}{2}\rho_{ba} - \frac{\Omega_p^*}{2}\rho_{ac}, \tag{A1h}$$

$$i\frac{\partial\rho_{bc'}}{\partial t} = \left[-i\left(\frac{\Gamma_{c'c}+\Gamma_{c'b}}{2} + \Gamma_{bc'}^{(\mathrm{ph})}\right) + (\delta_p - \delta_{c'})\right]\rho_{bc'} + \frac{\Omega_{c'}}{2}\rho_{ba} - \frac{\Omega_p^*}{2}\rho_{ac'}, \tag{A1i}$$

$$i\frac{\partial\rho_{cc'}}{\partial t} = -i\left(\frac{\Gamma_{cb}+\Gamma_{c'c}+\Gamma_{c'b}}{2} + \Gamma_{cc'}^{(\mathrm{ph})}\right)\rho_{cc'} + \frac{\Omega_{c'}}{2}\rho_{ca} - \frac{\Omega_c^*}{2}\rho_{ac'}. \tag{A1j}$$

Here, the three frequency detunings δ_c, $\delta_{c'}$, and δ_p are defined as follows: $\delta_c = \omega_c - \omega_{ac}$, $\delta_{c'} = \omega_{c'} - \omega_{ac'}$, and $\delta_p = \omega_p - \omega_{ab}$, where ω_{ac}, $\omega_{ac'}$, and ω_{ab} denote the energy-level transition frequencies, and ω_c, $\omega_{c'}$, ω_p represent the mode frequencies of the control and probe beams, respectively. $\Gamma_{ij}^{(\mathrm{ph})}$ denotes the dephasing rate. In order to analyze the characteristic of quantum coherence exhibited by the four-level system, we assume all the optical fields are on resonance, i.e., the frequency detunings δ_c, $\delta_{c'}$, and δ_p vanish and all the decay terms are temporarily ignored. It follows from Eq. (A1h) that $\rho_{ac} = \kappa\Omega_c$ and $\rho_{ba} = \kappa\Omega_p^*$, where κ is a parameter to be determined. In the same fashion, from Eq. (A1i), one can obtain $\rho_{ac'} = \lambda\Omega_{c'}$ and $\rho_{ba} = \lambda\Omega_p^*$, and from Eq. (A1j), the relations $\rho_{ca} = \varsigma\Omega_c^*$ and $\rho_{ac'} = \varsigma\Omega_{c'}$ can also yield. It can be easily seen that the three parameters are equal, $\kappa = \lambda = \varsigma$. Thus, we have the results,

$$\rho_{ab} = \varsigma\Omega_p, \quad \rho_{ac} = \varsigma\Omega_c, \quad \rho_{ac'} = \varsigma\Omega_{c'}. \tag{A2}$$

This solution agrees with Eqs. (A1a)–(A1d), if all the decay rates and frequency detunings vanish.

In order to treat the quantum coherence in the multilevel system, we will concentrate our attention on the equation of $\dot{\rho}_{ab}$, $\dot{\rho}_{cb}$, and $\dot{\rho}_{c'b}$. In Eqs. (A1e), (A1h), and (A1i), the terms related to the small quantities $\Omega_p\rho_{aa}$, $\Omega_p^*\rho_{ac}$, and $\Omega_p^*\rho_{ac'}$ can be ignored. Then we have the following complete set of equations

of $\{\rho_{ab}, \rho_{bc}, \rho_{bc'}\}$:

$$\begin{aligned}
\dot{\rho}_{ab} &= -(\gamma_{ab} - i\delta_p)\rho_{ab} + \frac{i}{2}\Omega_c\rho_{cb} + \frac{i}{2}\Omega_{c'}\rho_{c'b} + \frac{i}{2}\Omega_p\rho_{bb}, \\
\dot{\rho}_{cb} &= -[\gamma_{bc} - i(\delta_p - \delta_c)]\rho_{cb} + \frac{i}{2}\Omega_c^*\rho_{ab}, \\
\dot{\rho}_{c'b} &= -[\gamma_{bc'} - i(\delta_p - \delta_{c'})]\rho_{c'b} + \frac{i}{2}\Omega_{c'}^*\rho_{ab}. \qquad \text{(A3)}
\end{aligned}$$

where $\gamma_{ab} = \frac{\Gamma_{ac'}+\Gamma_{ab}+\Gamma_{ac}}{2} + \Gamma_{ab}^{(\mathrm{ph})}$, $\gamma_{bc} = \frac{\Gamma_{cb}}{2} + \Gamma_{bc}^{(\mathrm{ph})}$, and $\gamma_{bc'} = \frac{\Gamma_{c'c}+\Gamma_{c'b}}{2} + \Gamma_{bc'}^{(\mathrm{ph})}$. For the four-level system in the present paper, the levels $|b\rangle$, $|c\rangle$, $|c'\rangle$ have the same parity, and the spontaneous emission decay rates vanish, i.e., $\Gamma_{cb} = \Gamma_{c'c} = \Gamma_{c'b} = 0$. Then the dephasing rates dominate the decay rates γ_{bc} and $\gamma_{bc'}$, i.e., $\gamma_{bc} = \Gamma_{bc}^{(\mathrm{ph})}$ and $\gamma_{bc'} = \Gamma_{bc'}^{(\mathrm{ph})}$.

[1] A. M. Zheltikov, Phys. Rev. A **74**, 053403 (2006).
[2] A. Gandman, L. Chuntonov, L. Rybak, and Z. Amitay, Phys. Rev. A **75**, 031401(R) (2007).
[3] S. E. Harris, Phys. Today **50**, 36 (1997), and references therein.
[4] J. Q. Shen, *Classical & Quantum Optical Properties of Artificial Electromagnetic Media* (Transworld Research Network, Kerala, India, 2008).
[5] J. L. Cohen and P. R. Berman, Phys. Rev. A **55**, 3900 (1997).
[6] S. Y. Zhu and M. O. Scully, Phys. Rev. Lett. **76**, 388 (1996).
[7] C. Champenois, G. Morigi, and J. Eschner, Phys. Rev. A **74**, 053404 (2006).
[8] C. M. Krowne and J. Q. Shen, Phys. Rev. A **79**, 023818 (2009).
[9] J. Q. Yao, H. B. Wu, and H. Wang, Acta Sin. Quantum Opt. (China) **9**, 121 (2003).
[10] J. Q. Shen and P. Zhang, Opt. Express **15**, 6484 (2007).
[11] J. Q. Shen, New J. Phys. **9**, 374 (2007).
[12] E. Paspalakis and P. L. Knight, J. Opt. B: Quantum Semiclass. Opt. **4**, S372 (2002).
[13] E. Paspalakis and P. L. Knight, Phys. Rev. A **66**, 015802 (2002).
[14] A. Otto, Z. Phys. **216**, 398 (1968).
[15] E. Kretschmann, Z. Phys. **241**, 313 (1971).
[16] Y. Ding, Z. Q. Cao, and Q. S. Shen, Opt. Quantum Electron. **35**, 1091 (2003).
[17] A. V. Zayats, I. I. Smolyaninov, and A. A. Maradudin, Phys. Rept. **408**, 131 (2005).
[18] A. Ishimaru, S. Jaruwatanadilok, and Y. Kuga, Prog. Electrom. Res. **51**, 139 (2005).
[19] W. H. Weber and S. L. McCarthy, Phys. Rev. B **12**, 5643 (1975).
[20] L. E. Regalado, R. Machorro, and J. M. Siqueiros, Appl. Opt. **30**, 3176 (1991).
[21] J. Homola, S. S. Yee, and G. Gauglitz, Sensors Actuat. B **54**, 3 (1999).
[22] Y. Jiang, Z. Cao, G. Chen, X. Dou, and Y. Chen, Opt. Laser Technol. **33**, 417 (2001).
[23] P. Schuck, Annu. Rev. Biophys. Biomol. Struct. **26**, 541 (1997), and references therein.
[24] W. L. Barnes, A. Dereux, and T. W. Ebbesen, Nature (London) **424**, 824 (2003).
[25] E. Ozbay, Science **311**, 189 (2006).
[26] J. Yoon, S. H. Song, and J.-H. Kim, Opt. Express **16**, 1269 (2008).
[27] M. Davanço, P. Holmström, D. J. Blumenthal, and L. Thylén, J. Quantum Electronics **39**, 608 (2003).
[28] S. Marcinkevičius, A. Gushterov, and J. P. Reithmaier, Appl. Phys. Lett. **92**, 041113 (2008).
[29] J. Houmark, T. R. Nielsen, J. Mørk, and A.-P. Jauho, Phys. Rev. B **79**, 115420 (2009).
[30] J. M. Luther, P. K. Jain, T. Ewers, and A. P. Alivisatos, Nat. Mater. **10**, 361 (2011).
[31] R. Buonsanti, A. Llordes, S. Aloni, B. A. Helms, and D. J. Milliron, Nano Lett. **11**, 4706 (2011).
[32] M. Kanehara, H. Koike, T. Yoshinaga, and T. Teranishi, J. Am. Chem. Soc. **131**, 17736 (2009).
[33] M. O. Scully and M. S. Zubairy, *Quantum Optics* (Cambridge University Press, Cambridge, 1997).
[34] P. Yeh, *Optical Waves in Layered Media* (John Wiley & Sons, Somerset, 2005).
[35] C. Caloz and T. Itoh, *Electromagnetic Metamaterials: Transmission Line Theory and Microwave Applications* (John Wiley & Sons, Somerset, 2006).
[36] Z. Q. Cao, *Optics of Guided Waves* (Science Press of China, Beijing, 2007).
[37] P. Jänes, J. Tidström, and L. Thylén, J. Lightwave Technol. **23**, 3893 (2005).
[38] R. Mathew, C. E. Pryor, M. E. Flatté, and K. C. Hall, Phys. Rev. B **84**, 205322 (2011).
[39] P. Arve, P. Jänes, and L. Thylén, Phys. Rev. A **69**, 063809 (2004).
[40] J. Kim, S. L. Chuang, P. C. Ku, and C. J. Chang-Hasnain, J. Phys.: Condens. Matter **16**, S3727 (2004).
[41] P. K. Nielsen, H. Thyrrestrup, and B. Tromborg, Opt. Express **15**, 6396 (2007).
[42] R. Oshima, H. Komiyama, T. Hashimoto, H. Shigekawa, and Y. Okada, in *Conference Record of the (2006) IEEE 4th World Conference on Photovoltaic Energy Conversion*, Vol. 1 (IEEE, Washington, DC, 2006), pp. 158–161.
[43] L. E. Zohravi and M. Mahmoudi, Chin. Opt. Lett. **12**, 042601 (2014).
[44] H. Wang and K.-D. Zhu, Opt. Commun. **283**, 4008 (2010).
[45] A. L. Routzahn, S. L. White, L.-K. Fong, and P. K. Jain, Isr. J. Chem. **52**, 983 (2012).
[46] P. K. Jain, K. Manthiram, J. H. Engel, S. L. White, J. A. Faucheaux, and A. P. Alivisatos, Angew. Chem. Int. Ed. **52**, 13671 (2013).
[47] J. A. Faucheaux, A. L. D. Stanton, and P. K. Jain, J. Phys. Chem. Lett. **5**, 976 (2014).
[48] W. C. Martin and R. Zalubas, J. Phys. Chem. Ref. Data **10**, 153 (1981).
[49] I. Johansson, Ark. Fys. **20**, 135 (1961).

[50] C. J. Chang-Hasnain and S. L. Chuang, J. Lightwave Techn. **24**, 4642 (2006).

[51] S.-W. Chang, P. K. Kondratko, H. Su, and S. L. Chuang, IEEE J. Quantum Electron. **43**, 196 (2007).

[52] A. M. C. Dawes, L. Illing, S. M. Clark, and D. J. Gauthier, Science **308**, 672 (2005).

[53] M. Bajcsy, S. Hofferberth, V. Balic, T. Peyronel, M. Hafezi, A. S. Zibrov, V. Vuletic, and M. D. Lukin, Phys. Rev. Lett. **102**, 203902 (2009).

[54] Q. Xu, S. Sandhu, M. L. Povinelli, J. Shakya, S. Fan, and M. Lipson, Phys. Rev. Lett. **96**, 123901 (2006).